JOC The Journal of Organic Chemistry

Article

pubs.acs.org/joc

Bis(carbazolyl)ureas as Selective Receptors for the Recognition of Hydrogenpyrophosphate in Aqueous Media

Guzman Sanchez, Arturo Espinosa,* David Curiel, Alberto Tarraga, and Pedro Molina*

Departamento de Química Orgánica, Facultad de Química Campus de Espinardo, Universidad de Murcia, E-30100 Murcia, Spain

Supporting Information

ABSTRACT: Recognition properties of the novel bis(carbazole) tris-ureidic-based receptors **1** and **2** toward different anions have been studied by ^{1}H NMR and absorption and emission spectroscopy, as well as by DFT calculations. Receptor **1**, in which the two urea-functionalized arms are decorated with *p*-nitrophenyl rings, behaves as a highly selective chromogenic molecular probe for hydrogenpyrophosphate anion in a competitive medium (acetonitrile/water, 70/30). Receptor **2**, bearing two urea arms decorated with photoactive pyrenyl rings, acts as a highly selective fluorescent molecular probe for hydrogenpyrophosphate anion in either acetonitrile or an aqueous mixture (acetonitrile/water, 85/15). Receptor **2** exhibits a dual monomer−excimer emission spectrum and undergoes a remarked ratiometry in acetonitrile in the presence of hydrogenpyrophosphate: the excimer band disappears, whereas the monomer band is slightly increased. However, in the aqueous mixture, a strong increase of the excimer emission band was observed, while the monomer emission bands remained almost unaffected. The resulting binding modes and spectroscopic features are explained by suitable structures of model complexes for both receptors. In such complexes, a *peripheral cooperative effect* was found, alleviating the excess of negative charge in the guest toward the outer surface of the host, as well as the required enlargement on its internal cavity.

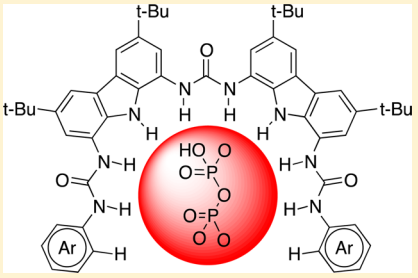

INTRODUCTION

In the field of supramolecular chemistry the topic of anion recognition and sensing has become an intense pursuit for a growing number of research groups worldwide.[1−5] Indeed, as a result of this effort, many excellent examples of hosts for anionic species have been successfully developed.[6−12]

Among anions, hydrogenpyrophosphate ($HP_2O_7^{3-}$) is a biologically important target because it plays an important role in energy transduction in organisms and controls metabolic processes by participation in enzymatic reactions. ATP hydrolysis, with the concomitant release of pyrophosphate, is central to many biochemical reactions, such as DNA polymerization and the synthesis of cyclic adenosine monophosphate (c-AMP) catalyzed by DNA polymerase and adenylate cyclase, respectively.[13−15] Furthermore, the detection of released pyrophosphate has been examined as a real-time DNA sequencing method,[16] and it has also been considered important in cancer research.[17] Telomerase (a biomarker for cancer diagnosis) activity is measured by evaluating the amount of pyrophosphate in the PCR amplification of the telomerase elongation product.[17] Furthermore, a high level of pyrophosphate in synovial fluids is correlated to calcium pyrophosphate dehydrate disease (CPDD), a rheumatologic disorder.[18,19] Therefore, the detection and discrimination of this anion has been the main focus of the effort of several research groups. However, very few examples of effective selective fluorescent,[20−30] chromogenic,[31−34] or redox[35] chemosensors have been reported so far. To date, several different heterocyclic ring systems containing a pyrrolic NH group have been reported in the literature as hydrogen-bond donors to anions, as demonstrated in calixpyrroles,[36−39] expanded porphyrinoids,[40,41] pyrrole derivatives,[42−45] indoles,[46] bis(indoles),[47] bis(imidazoles),[48−50] carbazole derivatives,[51−54] and imidazole derivatives.[55−58]

In this context, we report herein the design and sensing properties of the highly preorganized receptors **1** and **2** based on the bis(carbazolyl)urea scaffold[59−62] with a cavity suitable for the selective recognition of anionic species (Figure 1).

These anion receptors, which contain two carbazole rings and three urea subunits armed with chromogenic or fluorescent substituents, generate a cavity with eight well-oriented N−H groups pointing at the binding cavity. In this scaffold we combine the anion binding capabilities of the carbazole ring and the urea functionality[63−67] as well as the chromogenic properties of the *p*-nitrophenyl group[68] or the photophysical properties of the pyrene.[69]

RESULTS AND DISCUSSION

Synthesis. The synthesis of the target receptors **1** and **2** was carried out starting from 3,6-di-*tert*-butyl-9*H*-carbazole (**3**)[70,71] by a six-step procedure, as depicted in Scheme 1. When this alkylated carbazole was nitrated with the system fuming HNO_3/AcOH/Ac_2O, the dinitro derivative **4** was isolated in 40% yield. Despite the poor solubility of the latter compound, it was easily reduced with hydrazine, in the presence of palladium

Received: July 2, 2013
Published: September 11, 2013

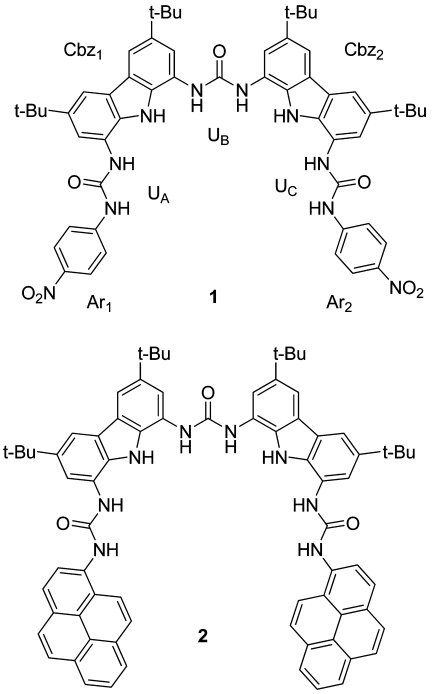

Figure 1. Structure of the receptors synthesized.

on charcoal as catalyst, to afford the corresponding diamine derivative **5** in excellent yield (93%). Controlled and selective N protection of **5** with Boc_2O provided the monoprotected derivative **6** in 40% yield. Treatment of this compound with *N*,*N*′-carbonyldiimidazole (CDI) led to the bis(carbazoyl)urea **7** in 67% yield, which was converted into the key intermediate **8**, in 80% yield, by treatment with trifluoroacetic acid. Finally, this compound was transformed into the target receptor **1**, in almost quantitative yield (98%), upon treatment with *p*-nitrophenyl isocyanate under standard conditions or into receptor **2** upon reaction with 1-pyrenyl isocyanate (prepared by a modification of the reported methods using biphosgene[72]), in good yield (Scheme 1).

Anion-Sensing Properties. *Receptor 1.* The anion recognition properties of the receptor **1** have been studied by using absorption techniques. The UV−vis absorption spectrum of receptor **1** in acetonitrile (2×10^{-5} M) (see the Supporting Information) exhibits three strong absorption bands located at λ 344 nm (ε = 72000 M^{-1} cm^{-1}), λ 297 nm (ε = 38000 M^{-1} cm^{-1}), and λ 229 nm (ε = 84000 M^{-1} cm^{-1}). The absorption spectrum of the receptor **1** displays noticeable changes only in the presence of hydrogenpyrophosphate anions. Titrations with this triply charged species induced the progressive appearance of two new absorption bands at λ 465 nm (ε = 27000 M^{-1} cm^{-1}) and λ 371 nm (ε = 61000 M^{-1} cm^{-1}), the new low energy (LE) band being responsible for the color change from colorless to yellow, which can be used for naked eye detection of this anion. The titration profile leveled off after the addition of 1 equiv of anion, and the Job plot confirmed the formation of a 1/1 complex due to the presence of a minimum value at a molar fraction of 0.5 (see the Supporting Information). From analysis of the spectral titration data the binding constant[73] was found to be log K_{11} = 6.50 ± 0.28 M^{-1}, and the detection limit[74] was 4.1×10^{-9} M. These preliminary experiments

Scheme 1. Synthesis of Receptors 1 and 2[a]

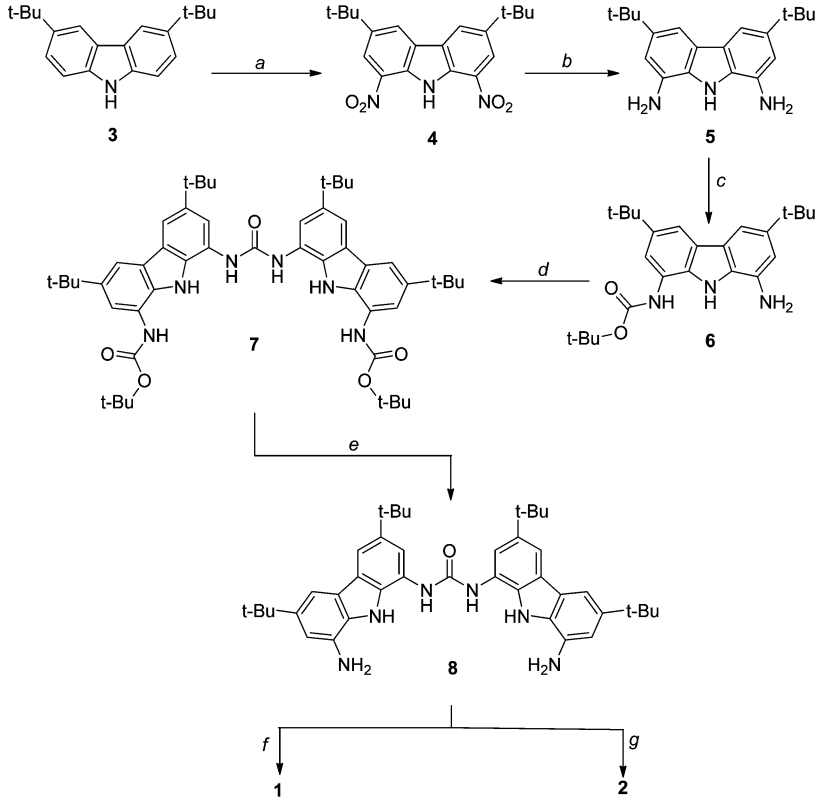

[a]Conditions (a) fuming HNO_3/AcOH/Ac_2O; (b) $N_2H_4{\cdot}H_2O$/Pd−C/EtOH; (c) Boc_2O/DCM; (d) CDI/DMF; (e) TFA/DCM; (f) 4-nitrophenyl isocyanate/THF; (g) 1-pyrenyl isocyanate/THF.

dx.doi.org/10.1021/jo401430d | J. Org. Chem. 2013, 78, 9725−9737

showed that, in a poorly competitive medium such as acetonitrile, receptor **1** can effectively bind $HP_2O_7^{3-}$.

In order to gain further understanding of the structure of the complex, ^{1}H NMR experiments in DMSO-d_6 were carried out.[75] Upon titration of receptor **1** with hydrogenpyrophosphate anion, all the aromatic signals shifted downfield (Figure 2). Unfortunately, with substoichiometric amounts of anion the

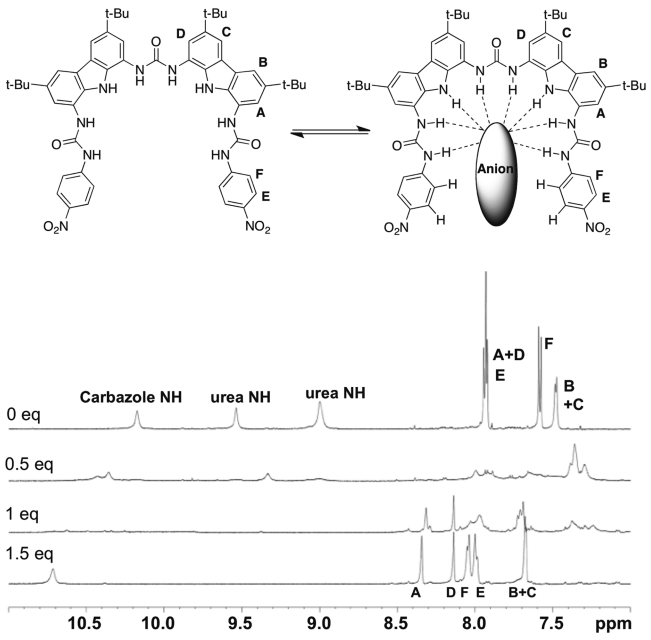

Figure 2. Evolution of the ^{1}H NMR spectra of receptor **1** in DMSO-d_6 upon addition of different aliquots of $HP_2O_7^{3-}$.

signals resulted extremely broadened, making its assignment impossible. Nevertheless, the signal shift ceased around 1 equiv of added guest and a new species started to be dominant since the signal became more readable, which might indicate that no further processes are taking place. These findings are consistent with the results obtained above by absorption spectroscopy, where the complex stoichiometry is 1/1.

The signals corresponding to the *p*-nitrophenylurea moieties (E and F) shifted downfield. This behavior could be understood by taking into account some significant interaction with the large pyrophosphate anion (see Theoretical Calculations). Moreover, signals corresponding to protons A–D also shifted downfield with increasing amounts of anion.

^{31}P NMR was used for further investigating the structure of the new species formed. For this purpose, a reverse titration, in which the hydrogenpyrophosphate anion was titrated with the receptor **1**, was performed in DMSO-d_6. As amounts of receptor **1** increased, the signal corresponding to the anion at δ −5.33 ppm was split into two resonances at δ −5.96 and −10.24 ppm that persisted along the rest of the titration and may indicate a loss in the magnetic equivalence of the anion, making both phosphorus atoms inequivalent (see the Supporting Information).

In order to increase the selectivity, water was added to the medium, ranging from 15 to 30% (v/v). Under these conditions, a different evolution in the absorption spectra was observed; the main difference with the noncompetitive medium was that no new bands above λ 400 nm were detected. Nevertheless, a modest increase of the absorption bands in the region of λ 370–400 nm was observed. Two isosbestic points were also detected at λ 364 and 281 nm, indicating the presence of a well-defined equilibrium between two species. Additionally, bands at λ 297 and 230 nm both underwent a decrease in their intensities. The titration profile followed the expected behavior for a recognition event leveling off after the addition of 1 equiv of anion (Figure 3).

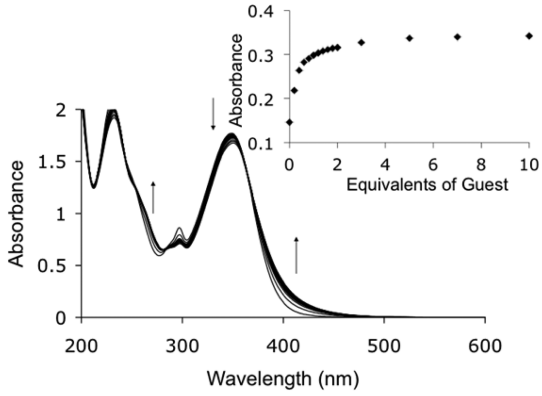

Figure 3. Evolution of absorption spectra of receptor **1** upon titration with $HP_2O_7^{3-}$ in 85/15 acetonitrile/water (v/v). Inset: binding isotherm at λ 400 nm.

The stoichiometry of the complex between receptor **1** and hydrogenpyrophosphate anion was confirmed by a Job plot analysis, which showed a minimum located around a molar fraction of 0.5. This result is in agreement with the formation of a 1/1 host/guest complex.

The incorporation of more water to the medium led to a slight decrease in the response, but it was still readable. Thus, up to 30% of water was added; as expected, the more water that was added, the more rounded the titration profile became due to the weakening of the interaction between host and guest. Nevertheless, in the most competitive situation studied (30% water), the titration profile still followed the expected behavior for a complexation event with a moderately high value in the constant (see the Supporting Information).

From the titration data, the corresponding binding constants[73] and detection limits[74] were calculated (see the Supporting Information). Even with an amount of water as high as 30%, the binding constant log K_{11} = 4.22 ± 0.10 M^{-1} is larger than 10000 and the detection limit 1.2 × 10^{-7} is in the submicromolar range.

Under these conditions, no positive response was detected for the other tested anions (acetate, benzoate, phthalate, isophthalate, terephthalate, trimesate, citrate, fluoride, chloride, bromide, iodide, cyanide, azide, dihydrogenphosphate, ADP, and ATP) (see the Supporting Information) making receptor **1** highly selective for hydrogenpyrophosphate anion. It is also remarkable that even citrate, a well-known strong competitor for $HP_2O_7^{3-}$ in sensing systems,[76] did not show a positive response.

Although the presence of water in the medium minimizes the possibility of having deprotonation,[77] hydrogenpyrophosphate is a basic anion, so that the recognition process may be confused with a deprotonation event or even a recognition/deprotonation equilibrium. In order to rule out this possibility, we performed a titration of **1** with the strong base tetrabutylammonium hydroxide, which clearly induces deprotonation as deduced from the different evolution of the absorption spectra (Figure 4).

dx.doi.org/10.1021/jo401430d | J. Org. Chem. 2013, 78, 9725–9737

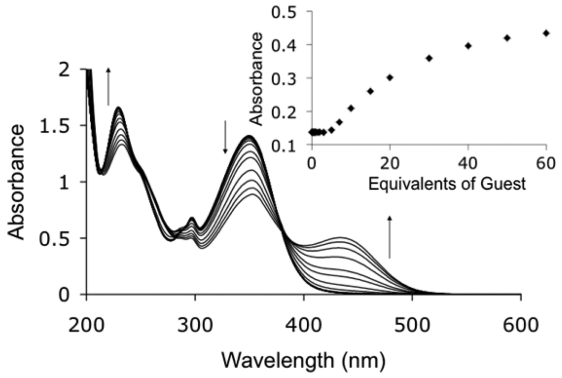

Figure 4. Evolution of absorption spectra of receptor **1** upon titration with TBAOH. Inset: titration isotherm at λ 400 nm.

In the first stages of the titration, no changes were observed in the spectra. Nevertheless, with a large excess of OH^- anion (ca. 5 equiv), the appearance of a new absorption band at λ 434 nm was detected together with a decrease in the intensity of the absorption bands of the receptor; in addition, an isosbestic point could be detected at λ 380 nm. The binding isotherm showed a sigmoidal shape. Moreover, addition of a large excess of anion (ca. 1000 equiv) did not affect the absorption spectrum of the complex (see the Supporting Information).

Furthermore, an NMR titration with tetrabutylammonium hydroxide (TBAOH) was carried out. Upon addition of base, the signals of all the NH groups in the molecule dissappeared. In addition, all the aromatic signals shifted upfield, as expected for a deprotonation process (see the Supporting Information). Therefore, these data ruled out the possibility of having a mere deprotonation process of the receptor **1** by the hydrogenpyrophosphate anion, indicating that the response observed is due to a dominant recognition event in solution.

Next, some competition assays were made in 80/20 acetonitrile/water. In the first place, a titration of receptor **1** with hydrogenpyrophosphate anion was carried out in the presence of 2 equiv of the rest of the anions (see the Supporting Information). The titration profile became more rounded and the initial slope resulted less abrupt, as expected due to the amount of interfering species in the medium. Moreover, 1 equiv of $HP_2O_7^{3-}$ was added to a solution containing 10 equiv of other interfering anions (see the Supporting Information). It is clear that even in the presence of large amounts of other species, the response toward $HP_2O_7^{3-}$ is kept. These competition experiments indicate that the complex is very stable and is formed even in the presence of a 10-fold excess of other anions.

The increase in the intensity of the absorption bands in the region λ 350−500 nm induced a color change, which allowed the naked-eye detection of hydrogenpyrophosphate (see the Supporting Information; only some anions shown as representative examples).

Receptor 2. The UV−vis spectrum of **2** exhibited two strong absorption bands at λ 349 nm (ε = 39000 $M^{-1}cm^{-1}$) and at λ 242 nm (ε = 112400 $M^{-1}cm^{-1}$) (see the Supporting Information). The addition of $HP_2O_7^{3-}$ caused the appearance of a new absorption band at λ 361 nm. Additionally, the presence of an isosbestic point at λ 310 nm was detected. As expected, the behavior of this receptor was very similar to that of **1**. The binding profile of **2** upon titration with $HP_2O_7^{3-}$ reached a saturation point after the addition of 1 equiv of anion. These findings suggest that a well-defined equilibrium exists between **2** and $HP_2O_7^{3-}$, giving a 1/1 complex (Figure 5). Binding assays using the method of continuous variations (Job

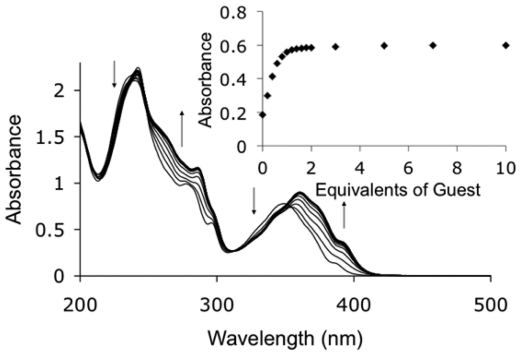

Figure 5. Evolution of the absorption spectra of receptor **2** upon titration with $HP_2O_7^{3-}$ in acetonitrile. Inset: titration profile at λ 380 nm.

plot) are consistent with a 1/1 (receptor/anion) binding stoichiometry, and from the absorption binding isotherm the association constant was calculated to be log K_{11} = 6.50 ± 0.28.

Assessment of the anion affinity also came from observing the extent to which the fluorescence intensity of the receptor **2** was affected in the presence of selected anions. Pyrenes display not only a well-defined monomer emission at 370−430 nm but also an efficient excimer emission at around 480 nm.[69] As the intensity ratio of excimer to monomer emission (I_E/I_M) is sensitive to the conformational changes of the pyrene-appended receptors, the I_E/I_M change upon ion complexation can be an informative parameter in various sensing systems. Receptor **2** displays in acetonitrile (c = 2 × 10^{-5} M) a dual spectrum (Figure 6), due to the presence of the two pyrene

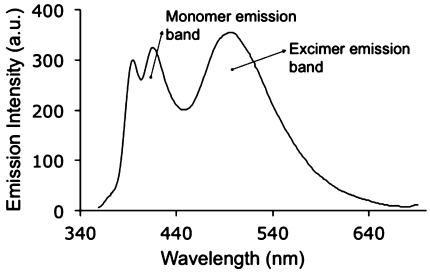

Figure 6. Emission spectrum of receptor **2** in acetonitrile (c = 2 × 10^{-5} M).

subunits, on excitation at λ_{exc} 345 nm. The emission spectrum of receptor **2** has a broad and red-shifted emission band at λ 496 nm, assigned to the excimer emission, and two additional and well-defined sharp bands at λ 416 and 394 nm arising from the monomer emission. The intensity ratio of excimer to monomer, I_E/I_M = 1.06, is barely changed in the concentration range of 10^{-7}−10^{-5} M, indicating that the excimer emission results from an intramolecular excimer but not from an intermolecular excimer. Consistently, increasing the solvent polarity by adding water had no effect on the maximum emission wavelength of the excimer emission band, indicating that the excited state did not possess any charge transfer character.[78]

It is important to emphasize the presence of a pyrene excimer emission band coexisting with the monomer emission bands. This could be explained either by an equilibrium of an

dx.doi.org/10.1021/jo401430d | J. Org. Chem. 2013, 78, 9725−9737

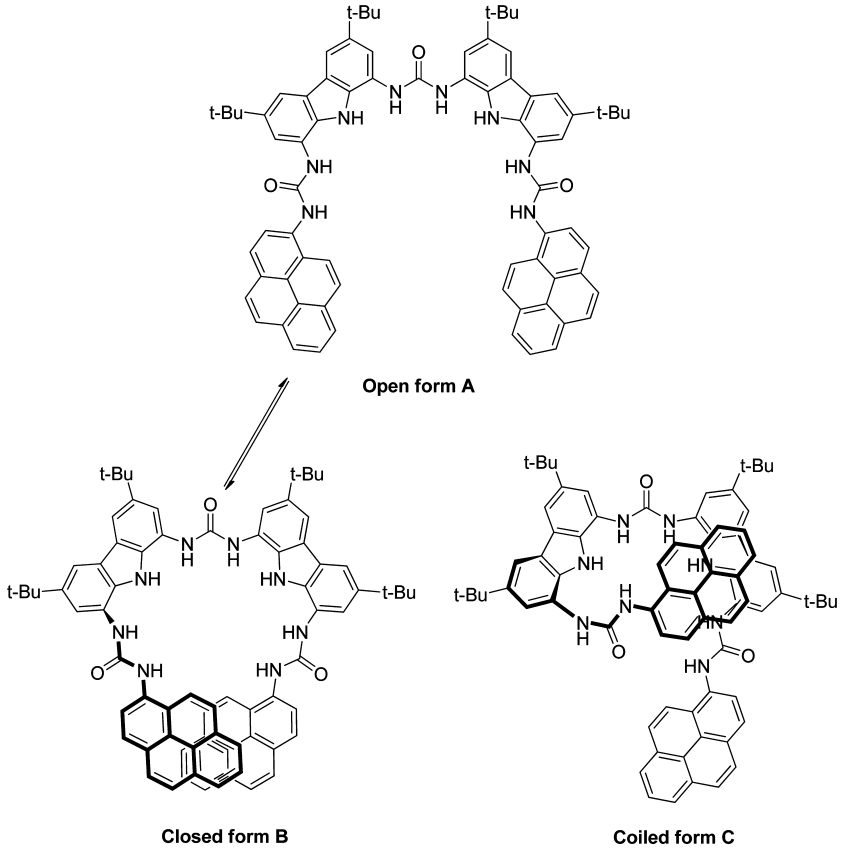

Figure 7. Possible conformations of receptor **2** in solution.

open form in which the two pyrenes are sufficiently remote to give only a monomer signal with the closed form B, in which the two pyrene units are overlapped favoring the formation of an excimer, closing the binding cavity, or by overlapping of one pyrene unit with a carbazole ring giving rise to the formation of an heteroexcimer emission band,[79] whereas the remaining pyrene unit is responsible for the monomer band, in the coiled form C (Figure 7).

Perturbation of the emission spectrum of receptor **2** in the presence of the aforementioned anions was also studied. Only addition of $HP_2O_7^{3-}$ anion induced a notable ratiometry, where the red-shifted structureless emission band dissapeared and the monomeric emission band at λ 394 nm is slightly red-shifted and increased (Figure 8). This result demonstrates that receptor **2** behaved as a ratiometric fluorescent probe for $HP_2O_7^{3-}$ without the interference of $H_2PO_4^-$ or the rest of the tested anions. The stoichiometry of the complex was determined by the changes in the fluorogenic response of receptor **2** in the presence of variyng concentrations of this anion, and the results indicate the formation of a 1/1 complex, with log K_{11} = 7.00 ± 0.57.

This behavior could be understood by taking into account that, while no anion is present, the receptor has its two side arms stacked, forming either an excimer or heteroexcimer between the pyrene groups or one pyrene and a carbazole group. However, the presence of the anion interacting with the binding cavity forces the side chains to open in order to accommodate the guest into the cavity, disabling any possibility of forming an intramolecular excimer. According to the results obtained by absorption and emission spectroscopy, a 1/1 stoichiometry was detected after the corresponding Job plot

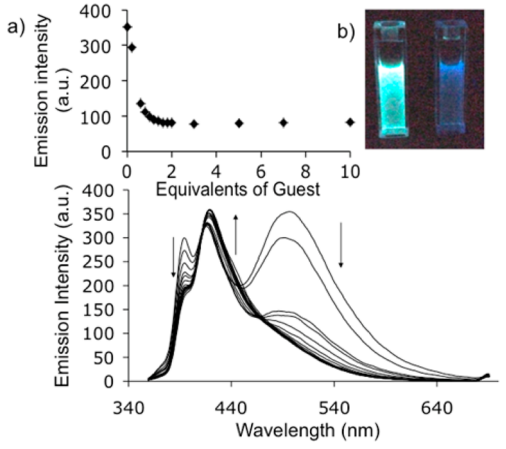

Figure 8. Evolution of the emission spectra of **2** upon titration with $HP_2O_7^{3-}$ in acetonitrile ($c = 2 \times 10^{-5}$ M). Insets: (a) binding isotherm at λ = 500 nm; (b) fluorescence color change upon addition of 1.5 equiv of $HP_2O_7^{3-}$ (left, **2** only; right, **2** + $HP_2O_7^{3-}$).

analysis, as was mentioned above (see the Supporting Information). ^{1}H NMR titrations were carried out in DMSO-d_6 due to the lack of solubility of **2** in acetonitrile or acetonitrile/water mixtures in the millimolar range, as occurred before with **1**. Upon addition of substoichiometric quantities of anion, all the signals broadened, suggesting the presence of a complex equilibrium system taking place in solution. Nevertheless, when 1 equiv of $HP_2O_7^{3-}$ was added, the signal shift ceased and the spectrum became perfectly resolved. No further changes were observed even when a large excess of anion was

dx.doi.org/10.1021/jo401430d | J. Org. Chem. 2013, 78, 9725−9737

added, supporting the formation of a 1/1 complex, according to the spectroscopic data (Figure 9).

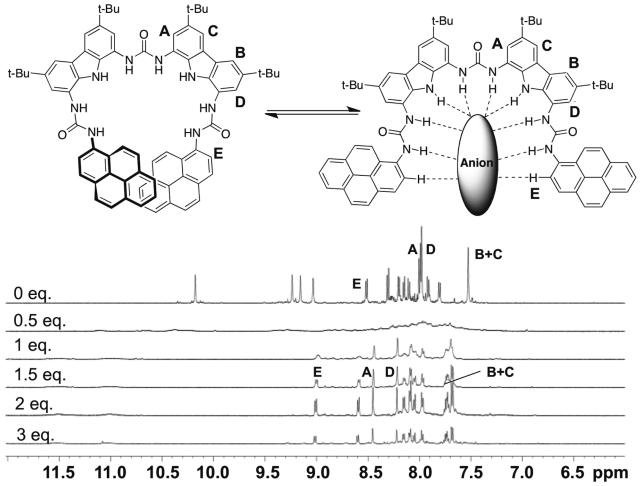

Figure 9. Evolution of the ^{1}H NMR spectra of **2**, in DMSO-d_6, upon titration with $HP_2O_7^{3-}$.

Again, all the signals of the carbazole moieties shifted downfield. As expected, the pyrene signals pointing outside the cavity shifted upfield, while those pointing into the cavity shifted downfield. It is important to note that the signal corresponding to the NH disappeared during the experiment.

Most remarkable is the fact that the spectroscopic response toward $HP_2O_7^{3-}$ is preserved in the presence of water. When this study was carried out in an aqueous environment (acetonitrile/water, 85/15), very small changes were detected in the absorption spectra upon titration with $HP_2O_7^{3-}$ (see the Supporting Information). The emission spectrum, however, underwent a completely different evolution in comparison to the results obtained in pure acetonitrile. Thus, a strong increase of the structureless emission band was observed, whereas the monomeric emission bands remained almost unaffected. Consequently, the intensity ratio of excimer to mononer I_E/I_M = 2.4 is more than 2-fold greater than that found in the free receptor (Figure 10).

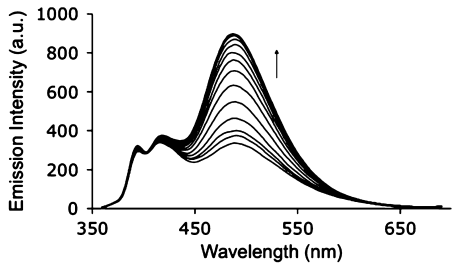

Figure 10. Evolution of fluorescence spectra of **2** upon titration with $HP_2O_7^{3-}$ in acetonitrile/water (85/15).

Since the saturation zone was reached after the addition of 2 equiv of $HP_2O_7^{3-}$, a Job analysis was carried out in order to check the stoichiometry of the complex. The Job plot has a minimum at around 0.33, which means that a complex with a stoichiometry of 1/2 (host/guest) was formed. This result differs from that obtained with **1** in the same medium; although the binding cavities are the same for both **1** and **2**, the former gave 1/1 complexes with $HP_2O_7^{3-}$ whereas the latter formed 1/2 complexes. Titration data could be satisfactorily fitted to a 1/2 model using the program SPECFIT/32, giving a constant value of log β_{12} = 13.60 ± 0.63 and a detection limit of 2.78 × 10^{-8} M. It is worth highlighting that the detection limit of **2** is of the same order of magnitude as that previously obtained for **1**.

Titrations with other anions showed slight or no interaction with the receptor, making this molecule very selective toward $HP_2O_7^{3-}$ (see the Supporting Information).

Titration of receptor **2** with TBAOH was also carried out in order to rule out the deprotonation process (see the Supporting Information). The fluorescence titration showed a behavior different from that observed in the case of $HP_2O_7^{3-}$. In this case, no enhancement of the excimer emission band was detected but a progressive decrease in its intensity followed by an abrupt quenching upon addition of a large excess of anion. On the other hand, the NMR spectra showed that all of the signals shifted upfield, with the exception of those corresponding to H_B and H_C. Additionally, some of the pyrene signals also shifted downfield. The difference between both $HP_2O_7^{3-}$ and TBAOH titrations permitted us to rule out the presence of a deprotonation process in the recognition process.

Theoretical Calculations. Quantum chemical calculations (see Computational Details) were undertaken to get a deeper insight into the nature of structural changes taking place in the aforementioned complexation processes and the spectroscopic features of both receptors and complexes. Model receptors **1a** and **2a** were used, which kept the entire framework but lacked just the peripheral *tert*-butyl groups, for the sake of computational efficiency. In both cases the most stable computed structures display a strongly coiled conformation with two consecutive urea (U_A and U_B) carbonyl groups and both carbazole NH groups pointing inward and mutually interacting. The other urea moiety (U_C) is located with its NH groups inward and interacts with the other external urea (A) carbonyl O atom.

The large amount of individual NCIs (noncovalent interactions) of either HB (hydrogen bond) and π- or T-stacking nature account for the significant stability of these coiled conformations even in polar solvents. Relevant parameters related to NCI strength are collected in Table 1. In addition to interaction distances, bond number quantities such as LBO[80−82] (Löwdin bond order) and especially WBI[83] (Wiberg bond index) are commonly used for assesing bond strength in the full range between strong covalent bonds and weak NCIs.[56,57,84−98] Another approach to the bond strength problem comes from Bader's atoms in molecules (AIM) theory.[99−101] Within this framework the electron density $\varrho(\mathbf{r})$ at the bond critical points (BCP) has been previously used as a mesure of bonding strength for both intra-[32,102−108] and intermolecular interactions (or soft intramolecular contacts).[32,109−113] NCIs are conveniently visualized by RDG (reduced density gradient) isosurfaces (see the Supporting Information), which are colored over the range −0.2 (blue) < $\sin(\lambda_2)\cdot\varrho$ < 0.2 (red) au:[114] blue denotes strong attraction, green stands for a moderate interaction, and red indicates strong repulsion (steric clashes).

It is worth highlighting the computed most stable coiled conformation for **2a** (Figure 11b) that displays strong π-stacking between Cbz_2 and Ar_1 units (here Ar = pyrene; compare interaction strength values with those of **1a** in Table 1) aligned in an almost parallel fashion (angle between mean planes 6.8°) and separated by a typical contact distance. This

dx.doi.org/10.1021/jo401430d | J. Org. Chem. 2013, 78, 9725−9737

Table 1. Bond Distances (Å) and Bond Strength Related Parameters Computed[a] for Main NCIs in Model Receptors 1a and 2a

	NCI	distance	LBO	WBI	$\varrho(\mathbf{r})^b$
1a	$(U_A)O\cdots HN(U_C)$	1.849	0.160	0.041	3.29
		2.174	0.057	0.011	1.59
	$(U_A)O\cdots HN(Cbz_1)$	2.003	0.094	0.016	2.43
	$(U_B)O\cdots HN(Cbz_1)$	2.463	<0.05	0.003	1.01
	$(U_B)O\cdots HN(Cbz_2)$	1.837	0.166	0.037	3.51
	$Cbz_2\cdots Ar_1$[c]	3.183	<0.05	0.003	0.75
	$Ar_2H\cdots Cbz_1$[c]	2.786	<0.05	0.002	0.75
2a	$(U_A)O\cdots HN(U_C)$	1.932	0.116	0.028	2.68
		2.132	0.068	0.014	1.61
	$(U_A)O\cdots HN(Cbz_1)$	2.078	0.075	0.013	2.05
	$(U_B)O\cdots HN(Cbz_1)$	2.318	<0.05	0.006	1.27
	$(U_B)O\cdots HN(Cbz_2)$	1.899	0.140	0.029	3.05
	$Cbz_2\cdots Ar_1$[c]	3.417[d]	<0.05[e]	0.063[f]	2.28[g]
	$Ar_2H\cdots Cbz_1$[c]	2.757	<0.05	0.002	0.75

[a]B3LYP(-D3)/def2-TZVPP//$COSMO_{DMSO}$/B3LYP-D3/def2-TZVP basis set. [b]$\times 10^2$, in e/a_0^3. [c]Closest H···Ar or $Ar_1\cdots Ar_2$ contact. [d]Average distance between Ar_1 and Cbz_2 mean planes at their centroids. [e]Individual atom−atom pairwise interactions below the threshold. [f]Sum extended over all atom−atom pairwise interactions. [g]Sum of five BCPs.

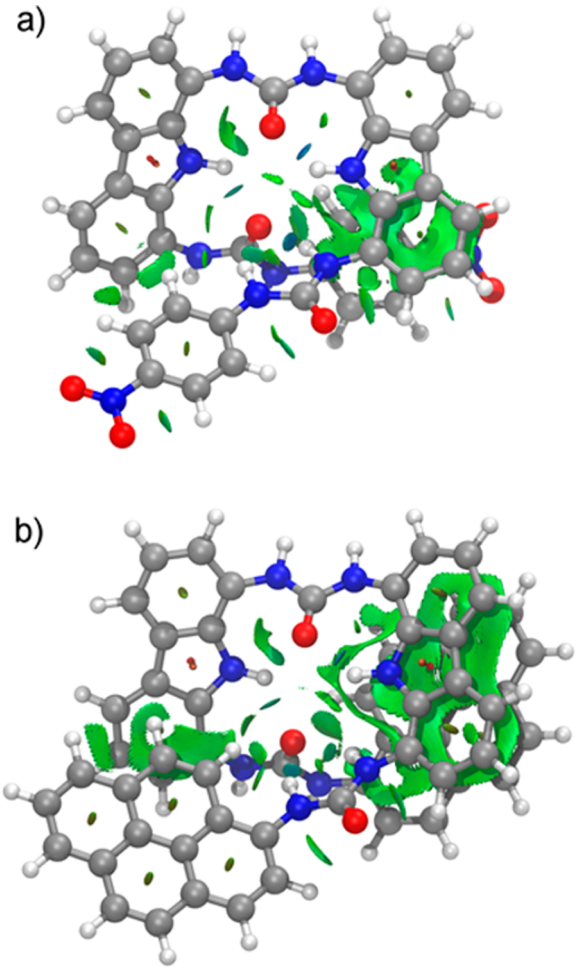

Figure 11. Calculated structures for model receptors **1a** and **2a**, showing NCI isosurfaces (0.04 isovalue) colored over the range $-0.2 < \sin(\lambda_2)\cdot\varrho < 0.2$ au.

remarkable structural feature fully supports the above proposed closed form B for receptor **2** (Figure 7) to explain the coexistence of a fluorescence emission band of pyrene monomer (the Ar_2 unit) together with an heteroexcimer emission originated by the $Cbz_2\cdots Ar_1$ pairing in the excited state.

Recognition of $HP_2O_7^{3-}$ anion by these receptors in the absence of water was modeled using receptor **1a** (the behavior of **2a** could be explained similarly) and assuming the experimentally found 1/1 receptor/anion stoichiometry. The most stable geometry in the PES (potential energy surface) of complex **1a**·$HP_2O_7^{3-}$ (two other slightly different relative minima were found) locates one "PO_4^{2-}" half of the hydrogenpyrophosphate anion (including the bridging O_b atom) roughly symmetrically wrapped by the central urea U_B unit, the carbazoles, and the directly connected NH groups of ureas U_A and U_C (Figure 12). The other "HPO_3^-" half of the anion is anchored by the two remaining urea NH groups and two ortho H atoms at the 4-nitrophenyl rings. In total, all eight NH groups form eight N−H···OP hydrogen bonds, which are supplemented by two additional Ar−H···OP interactions (Table 2). It is worth mentioning that complexation entails a deep conformational change around two out of three urea units: the OC−N−C1−C2 dihedral angles for the linkage of U_A and U_C to carbazole rings change from ap (or close to it) to sp conformation.

Moreover, the polarization of the urea N−H bonds upon complexation is efficiently delocalized toward the respective carbonyl O atoms that consequently become more electron rich, thus favoring internal HB formation with adjacent carbazole or phenyl (Ar_1) H atoms. Such polarization entails a *peripheral cooperative effect* of the outer convex part of the receptor when the inner concave surface is involved in complexation of the hydrogenpyrophosphate anion. This phenomenon promotes enlargement of the inner cavity by virtue of the peripheral H bonds being formed as a consequence of the electron density redistribution within the receptor: a significant portion of the negative charge of the anion is transferred to the receptor ($\Delta q^N = -0.324$ au), being mainly spread over the periphery (Figure 13, orange zones; $\Delta q^N = -0.327$ au), whereas the urea and carbazole N atoms (Figure 13, yellow zones; $\Delta q^N = -0.192$ au) can only partially compensate for the increase in positive charge at the H atoms they bear ($\Delta q^N = +0.273$ au). Despite these stabilizing interactions, the ligand strain amounts to 29.1 kcal/mol due to the large reorganization required for complexation starting from the receptor coiled structure. All these stabilizing effects together account for a large value of complexation energy of $\Delta E = -43.43$ kcal/mol (without BSSE correction).

The new set of peripheral HBs on complexation is in perfect agreement with the large downfield shift of the corresponding resonances observed in ^{1}H NMR (Figure 2, protons A, D, and F). Moreover, the computed ^{31}P chemical shifts for both phosphorus atoms P_1 (closest to the central U_A unit) and P_2 are −1.2 and −4.6 ppm (versus an in silico H_3PO_4 reference), respectively, pointing out their inequivalency in agreement with experimental observations (vide supra).

Finally, the complexation behavior of **2a** toward $HP_2O_7^{3-}$ anion in the presence of water was explored computationally. The key differential role played by water with respect to the studies in anhydrous solvents, together with the experimentally observed change in the stoichiometry to a 1/2 (receptor/anion) ratio, seems to suggest the consideration of (at least)

dx.doi.org/10.1021/jo401430d | J. Org. Chem. 2013, 78, 9725−9737

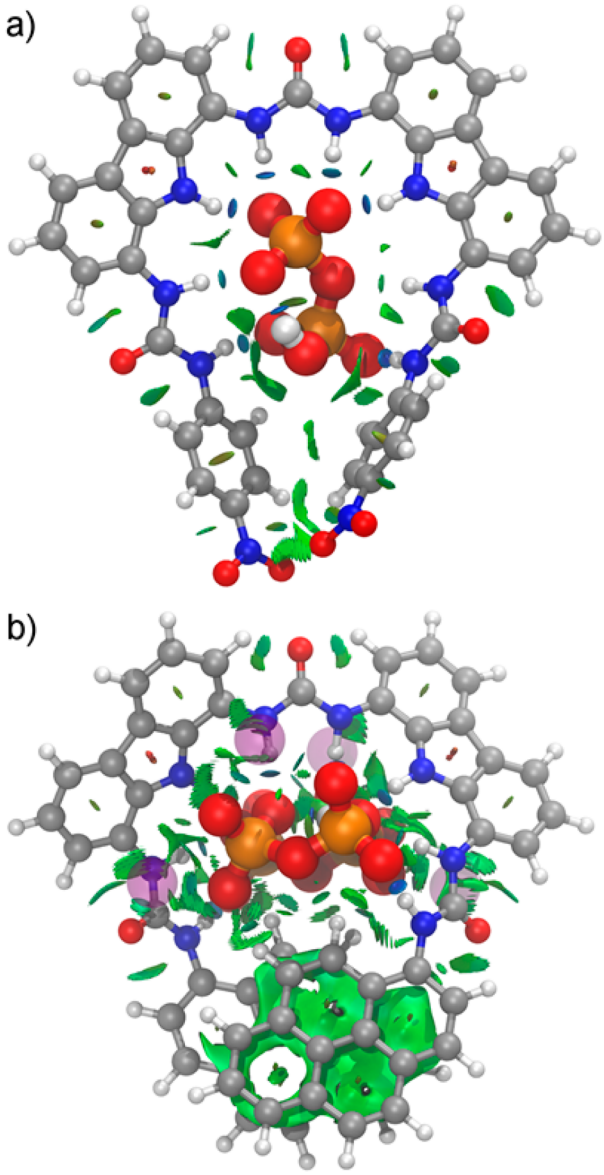

Figure 12. Calculated structures for model complexes (a) **1a**·($HP_2O_7^{3-}$) and (b) **2a**·(H_2O)($K_2HP_2O_7^-$)$_2$, showing NCI isosurfaces (0.04 isovalue). The host $HP_2O_7^{3-}$ units are drawn in a thicker ball and stick representation, with K^+ countercations (in b) as transparent violet spheres.

one explicit water molecule in a central position of the resulting complex. Indeed, a preliminary study showed that three water molecules can be conveniently hosted within the pseudocavity of receptor **2a**. In such a **2a**·(H_2O)$_3$ complex (see the Supporting Information) one H_2O guest molecule is bound to the NH groups of the central U_A unit, in a C_2-symmetrical fashion, thereby "opening" the coiled structure of the free receptor and positioning both terminal pyrene groups at π-stacking distance. The central H_2O guest molecule directs the O–H bonds to both sides of the new flat coiled arrangement of the receptor, thus favoring multisite interaction with two new H_2O molecules. Using this model, the molecular species resulting from the interaction of **2a** with hydrogenpyrophosphate in aqueous media was constructed by replacing the two external H_2O molecules by two anion units. To avoid the strong Coulombic repulsion between two highly negatively charged $HP_2O_7^{3-}$ species, the monoanionic $K_2HP_2O_7^-$ units were used instead for the modelization. The resulting **2a**·(H_2O)($K_2HP_2O_7^-$)$_2$ complex (Figure 12b) displays quasi-C_2 symmetry and features all eight NH groups pointing inward and an efficient pyrene–pyrene parallel stacking (interplanar angle 4.04°; distance at pyrene centroids 3.408 Å).

CONCLUSIONS

The neutral N–H-rich receptors **1** and **2** have been successfully synthesized from a key intermediate bis(aminocarbazolyl)urea derivative, which can be easily derivatized by reaction with isocyanates into the anion binding site urea unit capped by chromogenic or photoactive units. Recognition properties of these receptors toward different anions were studied by ^{1}H NMR, UV–vis, and emission spectroscopy. Both receptors display a high and selective affinity for the hydrogenpyrophosphate anion in aqueous mixtures. Receptor **1**, bearing terminal *p*-nitrophenyl rings in the two urea-functionalized arms, behaves as a highly selective molecular probe for hydrogenpyrophosphate anion either in acetonitrile or in a competitive medium (acetonitrile/water, 70/30): upon addition of this anion a modest increase of the absorption bands in the region λ 370–400 nm was observed, these perturbations being responsible for the color change from colorless to yellow. ^{31}P NMR data suggest a loss in the equivalence of phosphorus atoms in the anion, after binding with the receptor. Receptor **2**, with two photoactive pyrenyl rings, acts as a highly selective fluorescent molecular probe for hydrogenpyrophosphate anion in either acetonitrile or an aqueous mixture (acetonitrile/water, 85/15). Receptor **2**, which exhibits a dual emission spectrum, with monomer and excimer bands, underwent a remarked ratiometry in acetonitrile in the presence of hydrogenpyrophosphate: the excimer band disappears, whereas the monomer band is slightly increased, and the stoichiometry of the complex was found to be 1/1. The behavior of this receptor in an aqueous mixture (acetonitrile/water, 85/15), however, is quite different; a strong increase of the excimer emission band is observed, while the monomer emission bands remain almost unaffected, the stoichiometry of the complex changing to 1/2 (receptor/anion). With regard to the deprotonation/coordination dualism, absorption, emission, and NMR data strongly support that in both receptors the hydrogenpyrophosphate anion induces only hydrogen-bonded complex formation. DFT calculations supported the dual monomer/excimer emission behavior of receptor **2**, which could be explained by the most stable coiled conformer found that displays a pyrene–carbazole stacked pair together with an isolated nonstacked pyrene unit. Moreover, the calculated structures for complexes resulting upon interaction of hydrogenpyrophosphate anion with model receptors **1a** and **2a** fully agree with experimental NMR features and reveal the existence of a *peripheral cooperative effect*. Thus, complexation of the electron-rich $HP_2O_7^{3-}$ anion by **1a** entails an effective electron transfer to the outer surface of the receptor, through at least eight NCIs, which not only promotes alleviation of excess of negative charge at the guest but also enforces HB formation at the periphery of the host, which results in the required enlargement of the internal cavity. A model for the binding of **2a** with $HP_2O_7^{3-}$ anion in the presence of water, compatible with stoichiometry requirements and the inferred π-stacking interaction, is also proposed.

EXPERIMENTAL SECTION

General Remarks. Reagents used as starting materials were commercially available and were used without further purification.

dx.doi.org/10.1021/jo401430d | J. Org. Chem. 2013, 78, 9725–9737

Table 2. Bond Distances (Å) and Bond Strength Related Parameters Computed[a] for Main NCIs between Receptor and Anion in Model Complexes 1a·($HP_2O_7^{3-}$) and 2a·(H_2O)($HP_2O_7^{3-}$)

	NCI	distance	LBO	WBI	$\varrho(\mathbf{r})^b$
1a·($HP_2O_7^{3-}$)	$P_1O_1\cdots HN(U_B)$	1.769	0.227	0.064	4.14
	$P_1O_1\cdots HN(Cbz_1)$	1.769	0.224	0.063	4.17
	$P_1O_2\cdots HN(U_B)$	1.846	0.182	0.052	3.49
	$P_1O_2\cdots HN(Cbz_2)$	1.760	0.236	0.061	4.14
	$P_1O_3\cdots HN(U_A)$	1.889	0.177	0.044	3.06
	$PO_b\cdots HN(U_C)$	2.297	<0.05	0.007	1.15
	$P_2O_4\cdots HN(U_A)$	1.862	0.179	0.050	3.29
	$P_2O_4\cdots HC(Ar_1)$	2.423	<0.05	0.005	1.18
	$P_2O_5\cdots HN(U_C)$	1.754	0.237	0.071	4.30
	$P_2O_5\cdots HC(Ar_2)$	2.589	<0.05	0.003	0.83
intraligand	$(U_A)O\cdots HC(Ar_1)$	2.401	<0.05	0.002	1.37
	$(U_A)O\cdots HC(Cbz_1)$	2.164	0.062	0.006	2.02
	$(U_B)O\cdots HC(Cbz_1)$	2.265	<0.05	0.004	1.65
	$(U_B)O\cdots HC(Cbz_2)$	2.249	<0.05	0.004	1.70
	$(U_C)O\cdots HC(Cbz_2)$	2.534	<0.05	0.001	1.13
	$(U_C)O\cdots HC(Ar_2)$	2.321	<0.05	0.003	1.49
2a·(H_2O)($K_2HP_2O_7^-$)$_2$	$H_2O\cdots HN(U_B)$	1.872	0.161	0.039	3.15
		1.873	0.160	0.039	3.14
	$PO_b\cdots H_2O$	1.889	0.140	0.028	3.03
		1.894	0.138	0.028	3.00
	$PO_b\cdots H9_{Pyr}$	2.291	<0.05	0.003	1.45
		2.292	<0.05	0.003	1.45
	$P_1O_1\cdots HN(Cbz)$	2.051	0.096	0.022	2.28
		2.060	0.094	0.021	2.25
	$P_1O_1\cdots H8_{Pyr}$	2.387	<0.05	0.007	1.18
		2.406	<0.05	0.006	1.14
	$P_2O_5\cdots HN(U_{A/C})$	1.785	0.212	0.043	3.62
		1.787	0.211	0.043	3.60
		1.858	0.172	0.041	3.26
		1.864	0.169	0.040	3.21
intraligand	$(U_A)O\cdots HC(Ar_1)$	2.579	<0.05	0.001	[c]
		2.595	<0.05	0.001	[c]
	$(U_A)O\cdots HC(Cbz_1)$	2.634	<0.05	0.001	[c]
		2.634	<0.05	0.001	[c]
	$(U_B)O\cdots HC(Cbz_1)$	2.329	<0.05	0.003	1.50
		2.332	<0.05	0.003	1.50
	$Ar_i\cdots Ar_2$	3.408[d]	<0.05[e]	0.089[f]	2.66[g]

[a]B3LYP(-D3)/def2-TZVPP//$COSMO_{DMSO}$/B3LYP-D3/basis set. def2-TZVP was used for the optimization of **1a**·($HP_2O_7^{3-}$), whereas de2-SVP was used for **2a**·(H_2O)($K_2HP_2O_7^-$)$_2$. [b]$\times 10^2$, in e/a_0^3. [c]No BCP. [d]Average distance between Ar_1 and Cbz_2 mean planes at their centroids. [e]Individual atom−atom pairwise interactions below the threshold. [f]Sum extended over all atom−atom pairwise interactions. [g]Sum of five BCPs.

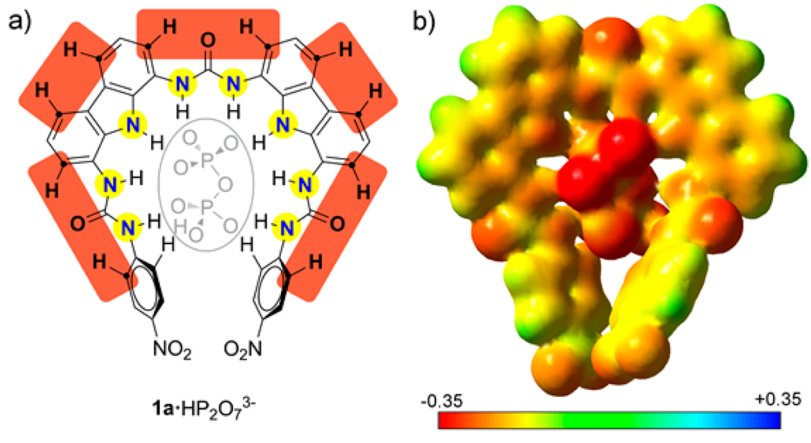

Figure 13. Enhancement of negative electric charge along the receptor **1a** on complexation: (a) sketch of partial deprotonation (yellow) and peripheral redistribution (orange); (b) electrostatic potential (in au) mapped onto a electron density isosurface (0.12 au).

dx.doi.org/10.1021/jo401430d | J. Org. Chem. 2013, 78, 9725−9737

Solvents were dried following the usual protocols (THF, Et_2O, and toluene were distilled from sodium wire with benzophenone indicator; CH_3CN and CH_2Cl_2 were distilled from $CaCl_2$; EtOH and MeOH were distilled from magnesium and stored with molecular sieves). Unless stated otherwise, all reactions were carried out under a nitrogen atmosphere. Column chromatography was run with silica gel 60 A CC 70−200 μm as the stationary phase with HPLC grade solvents. Melting points are not corrected. ^{1}H NMR, ^{13}C NMR, and NOESY experiments were recorded on 200, 300, 400, and 600 MHz instruments. Chemical shifts are referred to the residual peak of the solvent. In the experimental data "br" stands for a broad peak and "Cq" for a quaternary carbon atom. Mass spectrometry was recorded on an HPLC-MS TOF instrument using both positive and negative ionizations.

General Titration Protocol. Stock solutions were prepared with HPLC grade solvents. In the case of receptors **1** and **2**, 3 mL of a freshly prepared 2×10^{-5} M solutions was placed in a 1 cm cuvette and a UV or fluorescence spectrum was recorded. Then, aliquots of guest (all the anions as their tetrabutylammonium salts) were added and a spectrum was recorded immediately after each addition, giving a set of spectra showing the behavior of the receptor toward each analyte. The representation of data at a single wavelength against the anion concentration yields the binding isotherm. These plots were fitted using a nonlinear fitting algorithm provided by the computer program SPECFIT/32[73] in order to obtain the corresponding association constants and errors. The detection limits were set as the minimum concentration detectable at $S/N = 3$.[74]

1,8-Dinitro-3,6-di-*tert*-butyl-9*H*-carbazole (4). In a 500 mL round-bottom flask, **3** (900 mg, 3.23 mmol), acetic acid (3.05 mL), and acetic anhydride (2.30 mL) were added. The solution was then cooled to 1 °C, and fuming nitric acid (0.46 mL, 9.40 mmol) was added through an addition funnel. Once the addition of approximately $^1/_8$ of the whole volume of HNO_3 was complete, the cooling bath was replaced with an oil bath and the mixture was heated to 60 °C. Half of the remaining nitric acid was added under these conditions. During the addition of the rest of the HNO_3, the mixture was further heated to 75 °C. When the addition of acid was complete, the yellow suspension was heated to 110 °C and refluxed for 1 h. After this time, the suspended solid was filtered off and rinsed with boiling acetic acid. The yellow solid was further purified by crystallization in DMF. The extremely insoluble desired product was isolated as a yellow solid (500 mg, 40%). Mp: >300 °C. ^{1}H NMR (200 MHz, DMSO-d_6): δ (ppm) 1.47 (s, 18H), 8.37 (s, 2H), 9.06 (s, 2H), 11.10 (br, 1H). ^{13}C NMR: due to the lack of solubility of this compound, a carbon spectrum could not be recorded. HRMS (ESI-TOF): m/z $[M + H]^+$ ($C_{20}H_{24}N_3O_4$) found 370.1761, calcd 370.1689.

1,8-Diamino-3,6-di-*tert*-butyl-9*H*-carbazole (5). **4** (450 mg, 1.22 mmol) and Pd over activated carbon (100 mg) were suspended in EtOH under a nitrogen atmosphere. The mixture was heated to reflux, and hydrazine hydrate (3 mL, 50 mmol) dissolved in EtOH (10 mL) was added dropwise. The mixture was refluxed overnight until the solution turned colorless. The hot suspension was filtered through a Celite pad and was washed with EtOH. The filtrates were evaporated under reduced pressure, and the resulting solid was washed with hexane, yielding the desired product as a white crystalline solid (350 mg, 93%). Mp: 280−281 °C. ^{1}H NMR (200 MHz, DMSO-d_6): δ (ppm) 1.32 (s, 18H), 4.84 (br, 4H), 6.69 (d, 2H, J = 1.6 Hz), 7.24 (d, 2H, J = 1.6 Hz), 10.07 (s, 1H). ^{13}C NMR (50 MHz,, DMSO-d_6): δ (ppm) 32.0 (CH_3), 34.2 (Cq), 104.8 (CH), 107.5 (CH), 124.4 (Cq), 127.4 (Cq), 132.5 (Cq), 141.6 (Cq). HRMS (ESI-TOF): m/z $[M + H]^+$ ($C_{20}H_{28}N_3$) found 310.2280, calcd 310.2207.

***tert*-Butyl 8-Amino-3,6-di-*tert*-butyl-9*H*-carbazol-1-yl Carbamate (6).** *tert*-Butyl dicarbonate (200 mg, 0.91 mmol) was added dropwise to a solution of **5** (350 mg, 1.13 mmol) in dichloromethane (50 mL) at 0 °C. After the mixture was stirred overnight at room temperature, water was added (25 mL) and the biphasic mixture was extracted with CH_2Cl_2 (3 × 20 mL), dried with anhydrous Na_2SO_4, filtered, and evaporated, giving a light pink solid. This material was chromatographed in hexane/ethyl acetate 3/1 in order to remove the double-protected amine and then with hexane/AcOEt 1/1 for elution of the desired product. The product was isolated as a pinkish solid (150 mg, 40%). Mp: >300 °C. ^{1}H NMR (200 MHz, DMSO-d_6): δ (ppm) 1.33 (s, 9H), 1.36 (s, 9H), 1.50 (s, 9H), 5.01 (s, 2H), 6.73 (d, 1H, J = 1.2 Hz), 7.33 (d, 1H, J = 1.2 Hz), 7.57 (s, 1H), 7.73 (d, 1H, J = 1.4 Hz), 8.86 (br, 1H), 10.14 (s, 1H). ^{13}C NMR (75 MHz, DMSO-d_6): δ (ppm) 28.2 (CH_3), 31.9 (CH_3), 32.0 (CH_3), 34.3 (Cq), 34.4 (Cq), 79.0 (Cq), 104.7 (CH), 108.1 (CH), 111.6 (CH), 115.4 (CH), 122.4 (Cq), 122.9 (Cq), 124.3 (Cq), 127.4 (Cq), 132.7 (Cq), 140.7 (Cq), 142.2 (Cq), 153.3 (C═O). HRMS (ESI-TOF): m/z $[M + H]^+$ ($C_{25}H_{36}N_3O_2$) found 410.2812, calcd 410.2729.

1,3-Bis(3,6-di-*tert*-butyl-8-(*tert*-butoxycarbonylamino)-9*H*-carbazol-1-yl)urea (7). CDI (120 mg, 0.74 mmol) and **6** (400 mg, 0.98 mmol) were dissolved in dry DMF (30 mL) under a nitrogen atmosphere, and the mixture was stirred overnight at 60 °C. Then, the reaction was quenched with aqueous NaCl, affording a whitish precipitate. The desired compound was isolated pure by filtration in vacuo (400 mg, 67%). Mp: 188−190 °C. ^{1}H NMR (200 MHz, DMSO-d_6): δ (ppm) 1.38 (s, 18H), 1.40 (s, 18H), 1.44 (s, 18H), 7.48 (s, 2H), 7.78 (s, 2H), 7.84 (s, 2H), 7.91 (s, 2H), 8.78 (s, 2H), 9.27 (s, 2H), 10.23 (s, 2H). ^{13}C NMR (50 MHz, DMSO-d_6): δ (ppm) 28.1 (CH3), 31.8 (2xCH3), 34.5 (2 × Cq), 111.2 (CH), 112.1 (CH), 114.8 (CH), 117.0 (CH), 122.9 (2 × Cq), 123.9 (Cq), 124.2 (Cq), 129.7 (Cq), 131,6 (Cq), 141.5 (2 × Cq), 153.2 (C═O), 153.7 (C═O). HRMS (ESI-TOF): m/z $[M - H]^-$ ($C_{51}H_{67}N_6O_5$) found 843.5179, calcd 843.5252.

1,3-Bis(8-amino-3,6-di-*tert*-butyl-9*H*-carbazol-1-yl)urea (8). The bis(carbazolyl)urea species **7** (100 mg, 0.12 mmol) was dissolved in dichloromethane (20 mL), and trifluoroacetic acid (0.05 mL, 0.6 mmol) was added. The mixture was stirred at room temperature for 5 h. Then, the reaction was neutralized with an aqueous solution of $NaHCO_3$ (50 mL) and extracted with CH_2Cl_2. After drying, filtering, and evaporating, the resulting brown oil was dissolved in diethyl ether and gaseous HCl was bubbled through it. The grayish precipitate that formed was filtered off and washed with Et_2O (20 mL), affording the desired compound as a white solid (60 mg, 80%). Mp: 269−271 °C. ^{1}H NMR (200 MHz, DMSO-d_6): δ (ppm) 1.42 (m, 36H), 4.87 (br, 4H), 6.79 (s, 2H), 7.4 (m, 4H), 7.84 (s, 2H), 8.81 (s, 2H), 10.08 (s, 2H). ^{13}C NMR (50 MHz, DMSO-d_6): δ (ppm) 31.9 (CH_3), 34.3 (Cq), 104.9 (CH), 108.3 (CH), 112.1 (CH), 116.5 (CH), 122.77 (Cq), 123.4 (Cq), 124.8 (Cq), 127.5 (Cq), 131.8 (Cq), 132.1 (Cq), 140.9 (Cq), 142.2 (Cq), 153.9 (C═O). HRMS (ESI-TOF): m/z $[M + H]^+$ ($C_{41}H_{53}N_6O$) found 645.4276, calcd 645.4203.

1,3-Bis(8-(*p*-nitrophenylaminocarbonylamino)-3,6-di-*tert*-butyl-9*H*-carbazol-1-yl)urea (1). Diamine **8** (200 mg, 0.26 mmol) and commercially available *p*-nitrophenyl isocyanate (130 mg, 0.78 mmol) were dissolved in dry THF (30 mL), and the mixture was stirred at room temperature under a nitrogen atmosphere overnight. After this time, the solvent was evaporated and the resulting solid was further purified by column chromatography with AcOEt as eluent, yielding the desired compound as a yellow solid (250 mg, 98%). Mp: 287−289 °C. ^{1}H NMR (300 MHz, DMSO-d_6): δ (ppm) 1.35 (m, 36H), 7.45 (s, 4H), 7.56 (d, 4H, J = 9.3 Hz), 7.91 (m, 8H), 8.97 (m, 4H), 9.51 (s, 2H), 10.14 (s, 2H). ^{13}C NMR (75 MHz, DMSO-d_6): δ (ppm) 31.8 (CH_3), 34.4 (Cq), 111.9 (CH), 112.3 (CH), 116.3 (2xCH), 117.4 (CH), 122.2 (Cq), 123.3 (Cq), 124.5 (Cq), 124.9 (CH), 131.2 (Cq), 140.7 (Cq), 141.7 (Cq), 141.8 (Cq), 146.4 (Cq), 152.4 (Cq), 153.8 (C═O). HRMS (ESI-TOF): m/z $[M - H]^-$ ($C_{55}H_{59}N_{10}O_7$) found 971.4605, calcd 971.4646.

1,3-Bis(8-(pyrenylaminocarbonylamino)-3,6-di-*tert*-butyl-9*H*-carbazol-1-yl)urea (2). Diamine **8** (100 mg, 0.15 mmol) and 1-pyrenyl isocyanate (90 mg, 0.34 mmol) were dissolved in dry THF under a nitrogen atmosphere, and the mixture was stirred at room temperature for 24 h. Then, the solvent was evaporated and the residue was washed with ether, giving a grayish precipitate which corresponded with the analytically pure product (120 mg, 70%). Mp: >300 °C. ^{1}H NMR (200 MHz, DMSO-d_6): δ (ppm) 1.37−1.41 (m, 36H), 7.54 (m, 4H), 7.78−8.34 (m, 20H), 8.52 (d, 4H, J = 8.4 Hz), 9.06 (s, 2H), 9.20 (s, 2H), 9.27 (s, 2H), 10.20 (s, 2H). ^{13}C NMR (100 MHz, DMSO-d_6): δ (ppm) 31.8 (CH_3), 31.9 (CH_3), 34.4 (Cq), 34.5 (Cq), 111.9 (CH), 115.9 (CH), 116.3 (CH), 120.5 (CH), 121.1

dx.doi.org/10.1021/jo401430d | J. Org. Chem. 2013, 78, 9725−9737

(CH), 121.2 (Cq), 123.1 (Cq), 123.3 (Cq), 124.1 (CH), 124.3 (Cq), 124.4 (Cq), 124.7 (CH), 124.8 (Cq), 124.9 (CH), 125.2 (CH), 125.5 (Cq), 126.2 (CH), 126.4 (Cq), 126.6 (CH), 126.8 (CH), 127.2 (Cq), 130.5 (Cq), 131.0 (Cq), 131.1 (Cq), 131.2 (Cq), 132.9 (Cq), 141.9 (Cq), 153.5 (C═O), 153.9 (C═O). HRMS (ESI-TOF): m/z $[M + H]^+$ ($C_{75}H_{71}N_8O_3$) found 1131.5669, calcd 1131.5644.

Computational Details. Quantum chemical calculations were performed with the ORCA electronic structure program package.[115] All geometry optimizations were run with tight convergence criteria using the B3LYP[116,117] functional together with the new efficient RIJCOSX algorithm[118] and the def2-TZVP basis set,[119] except for the complex **2a**·$(H_2O)(K_2HP_2O_7^-)_2$, for which the basis set def2-SVP was used.[120] In all optimizations and energy evaluations, the latest Grimme semiempirical atom-pairwise correction (DFT-D3), accounting for the major part of the contribution of dispersion forces to the energy, was included.[121] Solvent effects (DMSO) were taken into account via the COSMO solvation model.[122,123] From these geometries all reported data were obtained by means of single-point (SP) calculations using the same functional as well as the more polarized def2-TZVPP[40,124] basis set. The topological analysis of the electronic charge density, $\varrho(\mathbf{r})$, was conducted using the AIM2000 software,[125] and the wave functions (electron densities) were generated with the Gaussian09 software package,[126] whereas for the NCIplot program the wave functions obtained with the def2-TZVP-f basis set were used as input. Reported energies are uncorrected for the zero-point vibrational term.

■ ASSOCIATED CONTENT

Supporting Information

Figures, text, and tables giving characterization data of all the new compounds, titrations in acetonitrile and in acetonitrile/water, fit plots, and molecular modeling data. This material is available free of charge via the Internet at http://pubs.acs.org.

■ AUTHOR INFORMATION

Corresponding Authors

*A.T.: e-mail, artuesp@um.es.

*P.M.: fax, +34 868 884 149; tel, +34 868 887 496; e-mail, pmolina@um.es.

Notes

The authors declare no competing financial interest.

■ ACKNOWLEDGMENTS

We acknowledge financial support from the MICINN of Spain and FEDER, project CTQ 2011-27175, Fundación Séneca Project 04509/GERM/06. G.S. also thanks the MICINN for a FPI fellowship.

■ REFERENCES

(1) Steed, J. W.; Gale, P. A. *Supramolecular Chemistry; From Molecules to Nanomaterials*; Wiley: Chichester, U.K., 2012.

(2) Vilar, R. Recognition of Anions. In *Structure and Bonding*; Mingos, D. M. P., Series Ed.; Springer Verlag: Berlin, 2008.

(3) Sessler, J. L.; Gale, P. A.; Cho, W.-S. *Anion Receptor Chemistry*; The Royal Society of Chemistry: Cambridge, U.K., 2006.

(4) Atwood, J. L.; Steed, J. W. *Encyclopedia of Supramolecular Chemistry*; Marcel Dekker: New York, 2004.

(5) Bianchi, A.; Bowman-James, K.; García-España, E. *Supramolecular Chemistry of Anions*; Wiley-VCH: New York, 1997.

(6) Wenzel, M.; Hiscock, J. R.; Gale, P. A. *Chem. Soc. Rev.* **2012**, *41*, 480.

(7) Hargrove, A. E.; Nieto, S.; Zhang, T. Z.; Sessler, J. L.; Anslyn, E. V. *Chem. Rev.* **2011**, *111*, 6603.

(8) Moragues, M. E.; Martínez-Máñez, R.; Sancenon, F. *Chem. Soc. Rev.* **2011**, *40*, 2598.

(9) Kubik, S. *Chem. Soc. Rev.* **2010**, *39*, 3648.

(10) Caltaginore, C.; Gale, P. A. *Chem. Soc. Rev.* **2009**, *38*, 520.

(11) Kim, S. K.; Lee, D. H.; Hong, J. I.; Yoon, J. *Acc. Chem. Res.* **2009**, *42*, 23.

(12) Gunnlaugsson, T.; Glynn, M.; Tocci, G. M.; Kruger, P. E.; Pferffer, F. M. *Coord. Chem. Rev.* **2006**, *250*, 3094.

(13) Lipscombe, W. N.; Sträter, N. *Chem. Rev.* **1996**, *96*, 2375.

(14) Tabary, T.; Lu, J. *J. Immunol. Methods* **1992**, *156*, 55.

(15) Nyren, P. *Anal. Biochem.* **1987**, *167*, 235.

(16) Ronaghi, M.; Karamohamed, S.; Petterson, B.; Uhlem, M.; Nyren, P. *Anal. Biochem.* **1996**, *242*, 84.

(17) Xu, S.; He, M.; Yu, H.; Cai, X.; Tan, X.; Lu, B.; Shu, B. *Anal. Biochem.* **2001**, *299*, 188.

(18) Doherty, M.; Becher, C.; Regan, M.; Jones, A.; Ledingham, J. *Ann. Rheum. Dis.* **1996**, *55*, 432.

(19) Timms, A. E.; Zhang, Y.; Russell, R. G.; Brown, M. A. *Rheumatology* **2002**, *41*, 725.

(20) Fabbrizzini, L.; Marcotte, N.; Stomeo, F.; Taglietti, A. *Angew. Chem., Int. Ed.* **2002**, *41*, 3811.

(21) Gunnlaugsson, T.; Davis, A. P.; O'Brien, J. E.; Glynn, M. *Org. Lett.* **2002**, *4*, 2449.

(22) Lee, D. H.; Kim, S. Y.; Hong, J.-I. *Angew. Chem., Int. Ed.* **2004**, *43*, 4777.

(23) Kanekiyo, Y.; Naganawa, R.; Tao, H. *Chem. Commun.* **2004**, 1006.

(24) Cho, H. K.; Lee, D. H.; Hong, J.-I. *Chem. Commun.* **2005**, 1690.

(25) Jang, Y. J.; Jun, E. J.; Lee, Y. J.; Kim, Y. S.; Kim, J. S.; Yoon, J. *J. Org. Chem.* **2005**, *70*, 9603.

(26) McDonough, M. J.; Reynolds, A. J.; Lee, W. Y. G.; Jolliffe, K. A. *Chem. Commun.* **2006**, 2971.

(27) Bazzicalupi, C.; Biagini, S.; Bencini, A.; Faggi, E.; Giorgi, C.; Matera, I.; Valtancoli, B. *Chem. Commun.* **2006**, 4087.

(28) Lee, N. H.; Swamy, K. M. K.; Kim, S. K.; Kwon, J.-Y.; Kim, Y. S.; Kim, S.-J.; Yoon, Y. J.; Yoon, J. *Org. Lett.* **2007**, *9*, 242.

(29) Lee, H. L.; Xu, Z.; Kim, S. K.; Swamy, K. M. K.; Kwon, S.-K.; Lee, H. N.; Shantha Kumar, S. M.; Kim, J. S.; Yoon, J. *Tetrahedron Lett.* **2007**, *48*, 8683.

(30) Romero, T.; Caballero, A.; Tárraga, A.; Molina, P. *Org. Lett.* **2009**, *11*, 3466.

(31) Lee, D. H.; Im, J. H.; Son, S. U.; Young, K.; Hong, J.-I. *J. Am. Chem. Soc.* **2003**, *125*, 7752.

(32) Aldakov, D.; Anzenbacher, P., Jr *J. Am. Chem. Soc.* **2004**, *126*, 4752.

(33) Nishiyabu, R., Jr. *J. Am. Chem. Soc.* **2005**, *127*, 8270.

(34) Zapata, F.; Caballero, A.; Espinosa, A.; Tárraga, A.; Molina, P. *J. Org. Chem.* **2008**, *73*, 4034.

(35) Anzenbacher, P., Jr; Palacios, M. A.; Kursikova, K.; Márquez, M. *Org. Lett.* **2005**, *7*, 5027.

(36) Anzenbacher, P., Jr; Jursíková, K.; Sessler, J. L. *J. Am. Chem. Soc.* **2000**, *122*, 9350.

(37) Gale, P. A.; Anzenbacher, P., Jr; Sessler, J. L. *Coord. Chem. Rev.* **2001**, *222*, 57.

(38) Nielsen, K. A.; Cho, W.-S.; Jappesen, J. O.; Lynch, V. M.; Becher, J.; Sessler, J. L. *J. Am. Chem. Soc.* **2004**, *126*, 16296.

(39) Sessler, J. L.; Katayev, E.; Pantos, G. D.; Scherbakov, P.; Reshetova, M. D.; Khrustaev, V. N.; Lynch, V. M.; Ustynyuk, Y. A. *J. Am. Chem. Soc.* **2005**, *127*, 11442.

(40) Sessler, J. L.; Davis, J. M. *Acc. Chem. Res.* **2001**, *34*, 989.

(41) Sessler, J. L.; Camiola, S.; Gale, P. A. *Coord. Chem. Rev.* **2003**, *240*, 17.

(42) Lin, C.-I.; Selvi, S.; Fang, J.-M.; Chou, P.-T.; Kai, C. H.; Cheng, Y.-Y. *J. Org. Chem.* **2007**, *72*, 3537.

(43) Sessler, J. L.; Pantos, G. D.; Gale, P. A.; Light, M. E. *Org. Lett.* **2006**, *8*, 1593.

(44) Curiel, D.; Espinosa, A.; Más-Montoya, M.; Sánchez, G.; Tárraga, A.; Molina, P. *Chem. Commun.* **2009**, 7359.

(45) Gale, P. A. *Chem. Commun.* **2005**, 3761.

(46) Pfeffer, F. M.; Lin, K. F.; Sedgwick, K. J. *Org. Biomol. Chem.* **2007**, *5*, 1795.

(47) Chong, K.-J.; Moon, D.; Lah, M. S.; Jeong, K.-S. *Angew. Chem., Int. Ed.* **2005**, *44*, 7926.

(48) Causey, C. P.; Allen, W. E. *J. Org. Chem.* **2002**, *67*, 5963.
(49) Zapata, F.; Caballero, A.; Tárraga, A.; Molina, P. *J. Org. Chem.* **2010**, *75*, 162.
(50) Alfonso, M.; Tárraga, A.; Molina, P. *Org. Lett.* **2011**, *13*, 6432.
(51) Curiel, D.; Cowley, A.; Beer, P. D. *Chem. Commun.* **2005**, 236.
(52) Curiel, D.; Más-Montoya, M.; Sánchez, G.; Orenes, R. A.; Molina, P.; Tárraga, A. *Org. Biomol. Chem.* **2010**, *8*, 4811.
(53) Curiel, D.; Sánchez, G.; Ramirez de Arellano, C.; Tárraga, A.; Molina, P. *Org. Biomol. Chem.* **2012**, *10*, 1896.
(54) Curiel, D.; Sánchez, G.; Más-Montoya, M.; Tárraga, A.; Molina, P. *Analyst* **2012**, *137*, 5449.
(55) Kang, J.; Kim, H.-S.; Jang, D. O. *Tetrahedron Lett.* **2005**, *46*, 6079.
(56) Alfonso, M.; Espinosa, A.; Tárraga, A.; Molina, P. *Org. Lett.* **2011**, *13*, 2078.
(57) Alfonso, M.; Espinosa, A.; Tárraga, A.; Molina, P. *Chem. Commun.* **2012**, *48*, 6848.
(58) Molina, P.; Tárraga, A.; Otón, F. *Org. Biomol. Chem.* **2012**, *10*, 1711.
(59) Jiménez, M. D.; Alcázar, V.; Peláez, R.; Sanz, F.; Fuentes de Arriba, A. L.; Caballero, M. C. *Org. Biomol. Chem.* **2012**, *10*, 1181.
(60) Hiscock, J. R.; Caltaginore, C.; Light, M. E.; Hursthouse, M. B.; Gale, P. A. *Org. Biomol. Chem.* **2009**, *7*, 1781.
(61) Edwards, P. R.; Hiscock, J. R.; Gale, P. A.; Light, M. E. *Org. Biomol. Chem.* **2010**, *8*, 100.
(62) Edwards, P. R.; Hiscock, J. R.; Gale, P. A. *Tetrahedron Lett.* **2009**, *50*, 4922.
(63) Choi, K.; Hamilton, A. D. *Coord. Chem. Rev.* **2003**, *240*, 101.
(64) Amendola, V.; Esteban-Gómez, D.; Fabbrizzi, L.; Licchelli, M. *Acc. Chem. Res.* **2006**, *39*, 343.
(65) Amendola, V.; Fabbrizzi, L.; Mosca, L. *Chem. Soc. Rev.* **2010**, *39*, 3889.
(66) Li, A.-F.; Wang, J.-H.; Wang, F.; Jiang, Y.-B. *Chem. Soc. Rev.* **2010**, *39*, 3729.
(67) Hossain, A.; Begum, R. A.; Rowshan, S.; Day, V. W.; Bowman-James, K. *Supramol. Chem.: Mol. Nanomater.* **2012**, *3*, 1153.
(68) Sola, A.; Orenes, R. A.; García, M. A.; Claramunt, R. M.; Alkorta, I.; Elguero, J.; Tárraga, A.; Molina, P. *Inorg. Chem.* **2011**, *50*, 4212.
(69) Winnick, F. M. *Chem. Rev.* **1993**, *93*, 587.
(70) Liu, Y.; Nishiura, M.; Wang, Y.; Hou, Z. *J. Am. Chem. Soc.* **2006**, *128*, 5592.
(71) Lai, W.-Y.; He, Q.-Y.; Chen, D.-Y.; Huan, W. *Chem. Lett.* **2008**, *37*, 986.
(72) Masse, C. E.; Van der Weide, K.; Kim, W. H.; Jiang, X. L.; Kumar, J.; Tripathy, S. K. *Chem. Mater.* **1995**, *7*, 904.
(73) Specfit/32 Global Analysis System, 1999−2004 Spectrum Software Associates (SpecSoft@compuserve.com). The Specfit program was adquired from Biologic, SA (www.bio-logic.info,) in January 2005. The equation to be adjusted by nonlinear regression, using the aforementioned software, was as follows: $\Delta A/b = \{K_{11}\Delta\varepsilon_{HG}[H]_{tot}[G]\}/\{1 + K_{11}[G]\}$, where H = host, G = guest, HG = complex, ΔA = variation in the absorption, b = cell width, K_{11} = association constant for a 1/1 model, and $\Delta\varepsilon_{HG}$ = variation of molar absorptivity.
(74) Shortreed, M.; Kopelman, R.; Kuhn, M.; Hoyland, B. *Anal. Chem.* **1996**, *68*, 1414.
(75) DMSO instead of acetonitrile/water was employed due to the lack of solubility of the receptor within the millimolar range.
(76) (a) Mizukami, S.; Nagano, T.; Urano, Y.; Odani, A.; Kikuchi, K. *J. Am. Chem. Soc.* **2002**, *124*, 3920. (b) Huang, F.; Cheng, C.; Feng, G. *J. Org. Chem.* **2012**, *77*, 11405.
(77) Duke, R. M.; O'Brien, J. E.; McCabe, T.; Gunnlaugsson, T. *Org. Biomol. Chem.* **2008**, *6*, 4089.
(78) Fages, F.; Desvergne, J.-P.; Bouas-Laurent, H. *J. Am. Chem. Soc.* **1989**, *111*, 96.
(79) Ghosh, D.; Nandi, N.; Chattopadhyay, N. *J. Phys. Chem. B* **2012**, *116*, 4693.
(80) Löwdin, P.-O. *J. Chem. Phys.* **1950**, *18*, 365.
(81) Lowdin, P.-O. *Adv. Quantum Chem.* **1970**, *5*, 180.
(82) Szabo, A.; Ostlund, N. S. *Modern Quantum Chemistry. Introduction to Advanced Electronic Structure Theory*; Dover Publications: Mineola, NY, 1989.
(83) Wiberg, K. B. *Tetrahedron* **1968**, *24*, 1083.
(84) Noor, A.; Glatz, G.; Müller, R.; Kaupp, M.; Demeshko, S.; Kempe, R. *Nat. Chem.* **2009**, *1*, 322.
(85) Schreiner, P. R.; Reisenauer, H. P.; Romanski, J.; Mloston, G. *Angew. Chem., Int. Ed.* **2009**, *48*, 8133.
(86) Helten, H.; Fankel, S.; Feier-Iova, O.; Nieger, M.; Espinosa, A.; Streubel, R. *Eur. J. Inorg. Chem.* **2009**, 3226.
(87) Otón, F.; Ratera, I.; Espinosa, A.; Wurst, K.; Parella, T.; Tárraga, A.; Veciana, J.; Molina, P. *Chem. Eur. J.* **2010**, *16*, 1532.
(88) Braunschweig, H.; Radacki, K.; Schwab, K. *Chem. Commun.* **2010**, *46*, 913.
(89) Epping, J. D.; Yao, S.; Karni, M.; Apeloig, Y.; Driess, M. *J. Am. Chem. Soc.* **2010**, *132*, 5443.
(90) Romero, T.; Orenes, R.-A.; Espinosa, A.; Tárraga, A.; Molina, P. *Inorg. Chem.* **2011**, *50*, 8214.
(91) Sola, A.; Otón, F.; Espinosa, A.; Tárraga, A.; Molina, P. *Dalton Trans.* **2011**, *40*, 12548.
(92) Otón, F.; González, M. C.; Espinosa, A.; Tárraga, A.; Molina, P. *Organometallics* **2012**, *31*, 2085.
(93) Alfonso, M.; Contreras-García, J.; Espinosa, A.; Tárraga, A.; Molina, P. *Dalton Trans.* **2012**, *41*, 4437.
(94) Espinosa, A.; Gómez, C.; Streubel, R. *Inorg. Chem.* **2012**, *51*, 7250.
(95) Espinosa, A.; Streubel, R. *Chem. Eur, J.* **2012**, *18*, 13405.
(96) Schulten, C.; von Frantzius, G.; Schnakenburg, G.; Espinosa, A.; Streubel, R. *Chem. Sci.* **2012**, *3*, 3526.
(97) Romero, T.; Espinosa, A.; Tárraga, A.; Molina, P. *Supramol. Chem.* **2012**, *24*, 826.
(98) Naskar, S.; Butcher, R.; Corbella, M.; Espinosa, A.; Chattopadhyay, S. K. *Eur. J. Inorg. Chem.* **2013**, 3249.
(99) Bader, R. F. W. *Atoms in Molecules: A quantum Theory*; Oxford University Press: Oxford, 1991.
(100) Bader, R. F. W. *Chem. Rev.* **1991**, *91*, 893.
(101) Matta, C. F.; Boyd, R. J. *The Quantum Theory of Atoms in Molecules*; Wiley-VCH: New York, 2007.
(102) Ran, J.; Wong, M. W. *Aust. J. Chem.* **2009**, *62*, 1062.
(103) Wang, H.; Csizmadia, I. G.; Marsi, I.; Chasse, G. A.; Fang, D.; Viskolcz, B. *J. Chem. Phys.* **2009**, *131*, 03505/1.
(104) Otón, F.; Espinosa, A.; Tárraga, A.; Ratera, I.; Veciana, J.; Molina, P. *Inorg. Chem.* **2009**, *48*, 1566.
(105) Raissi, H.; Jalbout, A. F.; Abbasi, B.; Fazli, F.; Farzad, F.; Nadim, E.; de León, A. *Int. J. Quantum Chem.* **2010**, *110*, 893.
(106) Ruíz, J.; Vicente, C.; de Haro, C.; Espinosa, A. *Inorg. Chem.* **2011**, *50*, 2151.
(107) Ruíz, J.; Rodríguez, V.; Cutillas, N.; Espinosa, A.; Hannon, M. J. *Inorg. Chem.* **2011**, *50*, 9164.
(108) Ruíz, J.; Rodríguez, V.; Cutillas, N.; Samper, K. G.; Capdevila, M.; Palacios, O.; Espinosa, A. *Dalton Trans.* **2012**, *41*, 12847.
(109) Pérez, J.; Espinosa, A.; Galiana, J. M.; Pérez, E.; Serrano, J. L.; Aranda, M. A. G.; Insausti, M. *Dalton Trans.* **2009**, 9625.
(110) Pérez, J.; Espinosa, A.; Galiana, J. M.; Pérez, E.; Serrano, J. L.; Cabeza, A.; Aranda, M. A. G. *Eur. J. Inorg. Chem.* **2008**, 3687.
(111) Nowroozi, A.; Jalbout, A. F.; Roohi, H.; Khalilinia, E.; Sadeghi, M.; de León, A.; Raissi, H. *J. Quantum Chem.* **2009**, *109*, 1505.
(112) Khan, M. A. S.; Kesharwani, M. K.; Bandyopadhyay, T.; Gnguly, B. *J. Mol. Struct. (THEOCHEM)* **2010**, *944*, 132.
(113) Streubel, R.; Villalba-Franco, J. M.; Schnakenburg, G.; Espinosa, A. *Chem. Commun.* **2012**, *48*, 5986.
(114) (a) *NCIplot, version 1.1*; Department of Chemistry, Duke University, Durham, NC, 2011; http://www.chem.duke.edu/~yang/Software/softwareNCI.html. (b) Johnson, E. R.; Keinan, S.; Mori-Sánchez, P.; Contreras García, J.; Cohen, A. J.; Yang, W. *J. Am. Chem. Soc.* **2010**, *132*, 6498−6506. (c) Contreras García, J.; Johnson, E. R.; Keinan, S.; Chaudret, R.; Piquemal, J.-P.; Beratan, D. N.; Yang, W. *J.*

Chem. Theory Comput. **2011**, *7*, 625−632. Here, λ_2 stands for the second highest eigenvalue of the electron density Hessian matrix.
(115) Neese, F. *ORCA An ab initio, DFT and semiempirical SCF-MO package, Version 2.9.1*; Max Planck Institute for Bioinorganic Chemistry, D-45470 Mülheim/Ruhr, Germany, 2012; http://www.mpibac.mpg.de/bac/logins/neese/description.php. Neese, F. *WIREs Comput. Mol. Sci.* **2012**, *2*, 73−78.
(116) Becke, A. D. *J. Chem. Phys.* **1993**, *98*, 5648.
(117) Lee, C. T.; Yang, W. T.; Parr, R. G. *Phys. Rev. B* **1988**, *37*, 785.
(118) Neese, F.; Wennmohs, F.; Hansen, A.; Becker, U. *Chem. Phys.* **2009**, *356*, 98.
(119) Weigend, F.; Ahlrichs, R. *Chem. Phys.* **2005**, *7*, 3297.
(120) Schaefer, A.; Horn, H.; Ahlrichs, R. *J. Chem. Phys.* **1992**, *97*, 2571.
(121) Grimme, S.; Antony, J.; Ehrlich, S.; Krieg, H. *J. Chem. Phys.* **2010**, *132*, 154104.
(122) Klamt, A. *J. Phys. Chem.* **1995**, *99*, 2224.
(123) Klamt, A.; Schürmann, G. *J. Chem. Soc. Perkin Trans. 2* **1993**, *220*, 799.
(124) Schäfer, A.; Huber, C.; Ahlrichs, R. *J. Chem. Phys.* **1994**, *100*, 5829−5835. Basis sets may be obtained from the Basis Set Exchange (BSE) software and the EMSL Basis Set Library: https://bse.pnl.gov/bse/portal. Feller, D. *J. Comput. Chem.* **1996**, *17*, 1571−1586.
(125) (a) AIM2000 v. 2.0, designed by F. W. Biegler-König and J. Schönbohm; home page http://www.aim2000.de/. Biegler-König, F.; Schönbohm, J.; Bayles, D. J. *J. Comput. Chem.* **2001**, *22*, 545−559. (b) Biegler-König, F.; Schönbohm, J. *J. Comput. Chem.* **2002**, *23*, 1489−1494.
(126) Frisch, M. J.; Trucks, G. W.; Schlegel, H. B.; Scuseria, G. E.; Robb, M. A.; Cheeseman, J. R.; Scalmani, G.; Barone, V.; Mennucci, B.; Petersson, G. A.; Nakatsuji, H.; Caricato, M.; Li, X.; Hratchian, H. P.; Izmaylov, A. F.; Bloino, J.; Zheng, G.; Sonnenberg, J. L.; Hada, M.; Ehara, M.; Toyota, K.; Fukuda, R.; Hasegawa, J.; Ishida, M.; Nakajima, T.; Honda, Y.; Kitao, O.; Nakai, H.; Vreven, T.; Montgomery, J. A., Jr.; Peralta, J. E.; Ogliaro, F.; Bearpark, M.; Heyd, J. J.; Brothers, E.; Kudin, K. N.; Staroverov, V. N.; Kobayashi, R.; Normand, J.; Raghavachari, K.; Rendell, A.; Burant, J. C.; Iyengar, S. S.; Tomasi, J.; Cossi, M.; Rega, N.; Millam, N. J.; Klene, M.; Knox, J. E.; Cross, J. B.; Bakken, V.; Adamo, C.; Jaramillo, J.; Gomperts, R.; Stratmann, R. E.; Yazyev, O.; Austin, A. J.; Cammi, R.; Pomelli, C.; Ochterski, J. W.; Martin, R. L.; Morokuma, K.; Zakrzewski, V. G.; Voth, G. A.; Salvador, P.; Dannenberg, J. J.; Dapprich, S.; Daniels, A. D.; Farkas, Ö.; Foresman, J. B.; Ortiz, J. V.; Cioslowski, J.; Fox, D. J. *Gaussian 09, Revision A.02*; Gaussian, Inc., Wallingford, CT, 2009.